Check for updates

Original Research Article

Impact of *Lonicera japonica* Extract on Nerve Growth Factor and Inflammatory Pathways in a Mouse Modeling of Allergic Rhinitis

Pharmacognosy Magazine
22(3) 1040–1055, 2026
© The Author(s) 2025
Article reuse guidelines:
in.sagepub.com/journals-permissions-india
DOI: 10.1177/09731296251355171
journals.sagepub.com/home/phm

Zhifeng Deng[1], Ting Zhu[1], Xiaoting Tong[1], Wendan Shi[1], Yu Xu[1] and Minli Zhang[2]

Abstract

Background: Although *Lonicera japonica* extract (LJE) has been widely used in traditional medicine for treating conditions such as heat-clearing, detoxification, and anti-bacterial purposes, its specific effects on allergic rhinitis (AR) remain underexplored.
Objectives: This study aimed to elucidate how LJE influences nerve growth factor (NGF) levels and associated inflammatory pathways in AR modeling of mice.
Materials and Methods: Chlorogenic acid, a key component of LJE, was isolated and optimized using orthogonal experiments and chromatographic techniques. An AR mouse modeling was established and divided into three groups: control group (no treatment), modeling group (LJE intervention), and modeling control group (model control group, saline intervention). Post-intervention, AR symptoms were evaluated, and serum and nasal mucosa tissues were analyzed. Western blotting was used to measure levels of PI3K, AKT, and NF-κB p65 proteins. At the same time, enzyme-linked immunosorbent assays (ELISA) quantified NGF, tumor necrosis factor (TNF)-α, interferon (IFN)-γ, interleukin (IL)-4, and IL-10 in serum and nasal mucosal tissue.
Results: Chlorogenic acid was successfully extracted with optimal conditions being 70% ethanol, pH 5, a solvent-to-material ratio of 10:1, and an extraction time of 1.5 h. The AR symptoms in the modeling group and model control group were significantly more severe compared to the control group ($p < .05$). Treatment with LJE notably reduced symptom severity in the modeling group relative to the model control group ($p < .05$). Additionally, the levels of PI3K, AKT, and NF-κB p65 in nasal mucosal tissue of the modeling group were comparable to those in the control group and lower than in the model control group ($p < .05$). NGF, TNF-α, and IFN-γ levels in the modeling group and control group were significantly lower than those in the model control group ($p < .05$), while IL-4 and IL-10 levels were higher in the modeling group and control group compared to the model control group ($p < .05$).
Conclusion: LJE effectively reduced NGF expression and alleviated AR symptoms in a mouse model, potentially through regulation of PI3K/Akt and NF-κB signaling pathways. This highlights LJE's therapeutic potential for managing AR-related inflammation.

Keywords

Allergic rhinitis, inflammatory pathways, *Lonicera japonica* extract, NF-κB signaling, PI3K/Akt signaling

Received 28 October 2024; **revised** 28 January 2025; **accepted** 21 May 2025

Introduction

Allergic rhinitis (AR) is a common chronic inflammatory disease that affects a large global population and significantly reduces the quality of life of patients (Siddiqui et al., 2022). Its pathogenesis involves complex immune dysregulation and neuroimmune interactions, with the nerve growth factor (NGF) playing a pivotal role in these processes (Bousquet et al., 2020). Abnormal elevation of NGF levels exacerbates

Zhifeng Deng, Ting Zhu, and Xiaoting Tong have contributed equally to this work.

[1]Department of Otolaryngology—Head and Neck Surgery, Renmin Hospital of Wuhan University, Wuhan, Hubei, China

[2]Yaxin School of Nursing, Wuhan Institute of Design and Science, Wuhan, Hubei, China

Corresponding author:
Minli Zhang, Yaxin School of Nursing, Wuhan Institute of Design and Science, Wuhan, Hubei 430205, China.
E-mail: minlizhangwh@163.com

Creative Commons Non Commercial CC BY-NC: This article is distributed under the terms of the Creative Commons Attribution-NonCommercial 4.0 License (http://www.creativecommons.org/licenses/by-nc/4.0/) which permits non-Commercial use, reproduction and distribution of the work without further permission provided the original work is attributed as specified on the SAGE and Open Access pages (https://us.sagepub.com/en-us/nam/open-access-at-sage).

the inflammatory response, leading to increased nasal mucosal sensitivity and triggering a range of typical AR symptoms, such as itching, sneezing, rhinorrhea, and nasal congestion (Mengi et al., 2022). Currently, various treatment options are available for AR, however, limitations in efficacy and the presence of adverse effects persist. Therefore, identifying safe and effective treatment methods and drug targets is of paramount importance (Tu et al., 2020; Velasco et al., 2022).

Lonicera japonica Thunb. (honeysuckle), a traditional Chinese medicinal herb has a long history of use in the medical field. Modern scientific research indicated that honeysuckle contains various bioactive compounds, such as chlorogenic acid and luteolin, which endow it with notable anti-inflammatory, antioxidant, and immune-modulatory properties (Du et al., 2021; Liu et al., 2023; Wang et al., 2022). In the treatment of inflammation-related diseases, honeysuckle has demonstrated promising efficacy (Mengi et al., 2022). Its anti-inflammatory mechanisms primarily involve the inhibition of inflammatory cell activation and aggregation, as well as the reduction of pro-inflammatory mediators such as tumor necrosis factor (TNF)-α and IL-6. Research showed that the aqueous extract of honeysuckle leaves suppresses the formation of inducible nitric oxide synthase (iNOS), nitric oxide (NO), and pro-inflammatory cytokines, including IL-1β and TNF-α, in lipopolysaccharide (LPS)-activated BV2 cells (Kweon et al., 2024). In a study, honeysuckle significantly reduced IL-6 and TNF-α levels in patients with colitis (Zang et al., 2024). Additionally, research indicated that chlorogenic acid and honeysuckle can synergistically inhibit the production of IL-1 and IL-6 (Wang et al., 2022). Honeysuckle also demonstrates a stronger inhibitory effect on the expression of inflammatory factors such as IL-6, TNF-α, and IL-1β (Liu et al., 2024). Furthermore, honeysuckle has been found to inhibit cytokine storm syndrome induced by IL-6 (Liang et al., 2021). Gołba et al. (2020) reported that honeysuckle berries exhibit anti-cancer, anti-inflammatory, and antioxidant activities. Additionally, honeysuckle can regulate the function of immune cells and correct immune imbalances, thereby alleviating inflammatory responses. Numerous studies have demonstrated that *L. japonica* extract (LJE) or compound formulations containing honeysuckle have shown positive effects in the treatment of various inflammatory diseases, such as respiratory and skin inflammation. LJE has been widely used in traditional medicine for clearing heat, detoxifying, and exhibiting anti-inflammatory and anti-bacterial properties. Recent research has gradually uncovered its potential roles in neuroprotection and immune modulation. Specifically, in allergic diseases, LJE has shown promising therapeutic effects by regulating immune responses and the expression of inflammatory mediators (Zheng et al., 2024). The chemical characterization of honeysuckle polyphenols and their protective effects against ultraviolet B (UVB)-induced damage in HaCaT cells, through the modulation of the Nrf2/NF-κB signaling pathway has been highlighted (Guo et al., 2023). Piekarska et al. (2023) indicated that honeysuckle demonstrates significant antioxidant, cardioprotective, anti-inflammatory, neuroprotective, anti-cancer, and anti-diabetic functions. Golubev et al. (2022) suggested that honeysuckle berry extracts containing lignan ether-terpenoids and anthocyanins help alleviate symptoms during the intestinal phase of trypanosome infection. Additionally, LJEs have been shown to extend the lifespan and improve the healthspan of fruit fly models through their biological and antioxidant activities. These studies provide compelling evidence supporting the therapeutic application of LJE in the treatment of inflammation-related diseases.

Given the anti-inflammatory properties of honeysuckle and the inflammatory nature of AR, along with the critical role of NGF in its pathogenesis, we hypothesize that LJE may intervene in the development of AR by modulating NGF expression. This study aims to investigate the regulatory effect of LJE on NGF expression in a mouse model of AR and further elucidate its potential mechanisms of action, thereby providing new therapeutic options and a theoretical basis for the treatment of AR.

Materials and Methods

Extraction of Chlorogenic Acid from L. japonica

Experimental Design

The ethanol reflux method was employed to extract chlorogenic acid from *L. japonica*. An orthogonal experiment was conducted to evaluate the influence of various parameters on extraction efficiency. These parameters included ethanol concentration, extraction time, solvent-to-material ratio, and pH. The experimental conditions and results are detailed in Table 1.

Single-factor Analysis

Following the orthogonal experiment, a single-factor analysis was performed to identify the primary and secondary factors that most significantly affect the yield of chlorogenic acid.

Table 1. Parameters for Orthogonal Experiment.

Level	Ethanol Concentration (%)	Extraction Time (h)	Solvent-to-material Ratio	pH
1	20	0.5	8	1
2	40	1	12	3
3	70	1.5	14	5
4	90	2	16	7

The single-factor analysis focused on optimizing these key factors based on the best results obtained from the orthogonal experiment.

Extraction Procedure

L. japonica (A Guo Yao Yuan Trading Co., Ltd., China) was first ground using a herbal medicine crusher (Jingju Powder Technology, Jiangsu, China) and sieved through a 20-mesh filter. The ground material was then measured and placed into a designated extraction vessel. Ethanol was added to the vessel as the solvent, and the mixture was thoroughly shaken to ensure complete immersion of the plant material. The pH of the mixture was measured and adjusted as needed. The plant material was soaked for 8 h.

After soaking, the pH was further adjusted using dilute solutions of sulfuric acid (H_2SO_4) and sodium carbonate (Na_2CO_3). The mixture was then transferred to a conical flask and placed in a water bath connected to a condenser. The extraction was carried out with two rounds of heating. Following extraction, the solution was centrifuged at 2,000 rpm for 25 min to separate the liquid from the residue. The supernatant containing the extracted chlorogenic acid was collected, and the remaining residue was discarded.

Chlorogenic Acid Determination in the LJE

To determine the content of chlorogenic acid in the LJE, several steps were followed. First, a control solution was prepared by accurately weighing 10 mg of chlorogenic acid reference standard (Chengdu GlycoBio Technology Co., Ltd., China) and dissolving it in 50 mL of 50% methanol solution. From this solution, aliquots of 1, 3, 5, 7, and 9 mL were transferred to 25 mL volumetric flasks, which were then filled to the mark with 50% methanol and shaken thoroughly to prepare various standard solutions for analysis.

For the sample preparation, the extract was concentrated using a rotary evaporator until the relative density reached between 1.15 and 1.20. A 0.5 g portion of the concentrated LJE sample was dissolved in 50% methanol and transferred to a 25 mL volumetric flask. The solution was shaken well and then filtered through a 0.45 μm microporous membrane to remove any particulate matter.

High-performance liquid chromatography (HPLC) was then employed to analyze the prepared sample. The analysis was conducted using an Agilent Technologies HPLC system with a Phenomenex C_{18} chromatographic column (150 × 4.6 mm, 5 μm). The mobile phase consisted of a mixture of acetonitrile and 0.4% phosphoric acid solution in a ratio of 13:87. The detection was performed at a wavelength of 327 nm, with a flow rate of 1.0 mL/min, and a column temperature set at 30°C. A 20 μL aliquot of the sample was injected into the chromatograph. Data collection continued until the peak elution was complete, at which point the chromatographic peak area and mass spectrometric analysis results were reviewed. Each sample was analyzed in duplicate, and the difference between the peak areas of the two injections was required to be less than 1% to ensure accuracy; otherwise, the sample was re-injected.

The optimal extraction process identified in the previous experiments was validated by repeating it three times. The results from these repeated extractions were compared to assess the stability and reproducibility of the extraction method. This verification step ensured that the extraction process was consistent and reliable for determining chlorogenic acid content in the extract.

Modeling Establishment

In this study, 15 adult male C57BL/6 mice (21–23 days old with a body weight of 22 ± 0.4 g; Nanjing Pengsheng Biotechnology Development Co., Ltd., China) were selected. The mice were housed under standard laboratory conditions. Ten mice were randomly assigned to the experimental group, for the induction of AR. The remaining five mice were assigned to the control group and received saline instead of the AR-inducing treatment. All animal experiments were approved by the Animal Ethics Committee of Renmin Hospital of Wuhan University, in compliance with Chinese national guidelines for the care and use of animals.

Sensitization Protocol

Experimental group: Each mouse received an intraperitoneal injection of 20 μg of ovalbumin (Sigma–Aldrich Corporation, USA) and 32 mg of aluminum hydroxide ($Al(OH)_3$) dissolved in 200 μL of phosphate buffered solution (PBS, Wuhan PunoSai Life Technology Co., Ltd., China). This sensitization mixture was administered at a dose of 0.2 mL per mouse, once daily, for a total of seven consecutive days.

Control Group

Mice in this group were injected with 0.2 mL of a sensitization solution containing only $Al(OH)_3$, prepared in advance and administered intraperitoneally once daily for 7 days. The sensitization solution was prepared 3 days before administration and allowed to mix thoroughly overnight.

Beginning on the 15th day after completing the initial sensitization, the mice in both groups were subjected to intranasal stimulation with a 2 mg/mL solution of ovalbumin in PBS. Each nostril of the mice was treated with 10 μL of this ovalbumin solution once daily for a duration of 1 week.

Grouping and Intervention

The mice in the experimental group were further divided into two subgroups to evaluate the effects of different treatments. The two subgroups were as follows.

Modeling Group

Mice in this subgroup received oral administration of LJE solution with a concentration of 0.06 g/mL. Each mouse was given a daily dose of 0.5 mL of the LJE solution for a period of 10 days.

Model Control Group

Mice in this subgroup were administered an equivalent volume of saline solution orally, following the same schedule as the modeling group.

The study involved a systematic approach to modeling establishment, sensitization, and intervention, allowing for a comprehensive evaluation of the effects of LJE on AR in mouse modeling.

Separation of Nasal Mucosa Tissue

Upon completion of the treatment regimen, the mice were administered a final intranasal ovalbumin challenge to induce AR symptoms. Mice were first anesthetized using 5% isoflurane, with an induction dose ranging from 2% to 3% (v/v) and an oxygen flow rate of 1–2 L/min. The mice were exposed to isoflurane for 1–2 min to achieve anesthesia, after which they were carefully positioned in a prone posture. To facilitate blood collection, the tail was immersed in warm water and then dried with a cotton ball. A disposable venous blood collection needle was inserted into the tail vein to draw blood. The blood was immediately transferred to a 1.5 mL Eppendorf tube and allowed to stand at room temperature for 1 h to promote coagulation. Subsequently, the samples were centrifuged at 12,000 rpm for 15 min at 4°C using a centrifuge (Thermo Fisher Scientific, USA). The serum was then carefully pipetted from the tube, and if the separation was incomplete, a second centrifugation was performed. The serum samples were immediately transferred to a liquid nitrogen container and subsequently stored at –80°C, ensuring they were not subjected to repeated freeze–thaw cycles.

After serum collection, the procedure for obtaining tissue specimens commenced. The mouse's abdomen was opened using scissors until the heart was exposed. A puncture needle was inserted into the left ventricle, and the right atrium was cut to allow for the drainage of blood. The heart was then perfused with chilled 0.9% physiological saline until the liver appeared pale, and the outflowing blood was clear, indicating that the blood had been effectively washed out. Following this, the fur from the mouse's nose was carefully trimmed with small scissors. The upper nasal bone was separated using scissors to expose the nasal dorsum, which was then split along the midline to reveal both nasal cavities and the nasal septum as completely as possible. The nasal mucosa was meticulously detached from the nasal septum, with all accessible tissue collected and placed into 1.5 mL Eppendorf tubes. These samples were immediately stored in a liquid nitrogen container and later transferred to a −80°C ultra-low-temperature freezer to preserve the tissue for future analysis, avoiding freeze–thaw cycles.

Assessment of AR Symptoms

During the final intranasal challenge, which marked the conclusion of the modeling phase, and within 30 min following the treatment, the mice were closely monitored for an additional 30 min to evaluate their AR symptoms. Observations focused on behaviors such as nasal scratching, nasal discharge (including tearing), and sneezing. These behaviors were scored based on the criteria outlined in Table 2.

Western Blotting

To investigate the involvement of PI3K/AKT and NF-κB signaling pathways in AR, Western blot analysis was used to measure the levels of PI3K (p-PI3K and t-PI3K), AKT (p-AKT and t-AKT), and NF-κB (p-NF-κB and t-NF-κB). The primary antibodies used were as follows. For the detection of PI3K/AKT signaling pathway-related proteins, the primary antibody against PI3K was derived from a rabbit (catalog number 4257S; Cell Signaling Technology, USA) and was diluted at a ratio of 1:1,000. The primary antibody for AKT was also derived from rabbit (catalog number ab8805; Abcam, UK) and was diluted at a ratio of 1:1,500. For the NF-κB signaling pathway, the primary antibody for NF-κB p65 was of mouse origin (catalog number sc-372; Santa Cruz Biotechnology, USA) and was diluted at a ratio of 1:800. For secondary antibodies, the corresponding secondary antibody for the aforementioned rabbit primary antibodies was goat anti-rabbit IgG-HRP (catalog number 111-035-003; Jackson Immuno Research, USA), diluted at a ratio of 1:5,000. The corresponding secondary antibody for the mouse primary antibody was goat anti-mouse IgG-HRP (catalog number 115-035-003; Jackson Immuno Research, USA), also diluted at a ratio of 1:5,000. All antibodies were validated for specificity and high performance, and their usage followed the manufacturer's recommendations. The blots were incubated with the primary antibody overnight at

Table 2. Scoring System for Allergic Rhinitis (AR) Symptoms.

Symptom	Score 0	Score 1	Score 2	Score 3
Nasal scratching	None	Rarely	Frequently	Constantly
Nasal discharge	None	Mild	Regulate	Severe
Sneezing	None	1–3 times	4–6 times	More than 6 times

4°C, followed by a 1-h incubation at room temperature with the secondary antibody.

Proteins were extracted from the nasal mucosa tissue of the mice and quantified. These protein extracts were separated using sodium dodecyl sulfate-polyacrylamide gel electrophoresis (SDS-PAGE) and transferred onto a polyacrylamide gel membrane (Millipore Corporation, USA). Target proteins were detected through immunoblotting with specific antibodies, followed by visualization using secondary antibodies conjugated with chemiluminescent or fluorescent markers. The resultant chemiluminescent or fluorescent signals were captured with an imaging system (Biolog Life Science Institute Co., Ltd., USA). The images were analyzed with specialized software to quantify the protein bands and assess their expression levels.

Assessment of NGF and Cytokines

To measure the levels of NGF, TNF-α, interferon (IFN)-γ, interleukin (IL)-4, and IL-10 in the serum, commercial enzyme-linked immunosorbent assays (ELISA) kits (Beijing Zhongshan Jinqiao Biotechnology Co., Ltd., China) were employed following the manufacturer's guidelines. Blank wells were used as controls, containing no samples or enzyme-conjugated reagents, while the test wells were prepared with 50 μL of serum sample mixed with 100 μL of enzyme-conjugated reagent. The plate was covered and incubated at 37°C for 60 min. Following incubation, the plate was washed five times with a washing buffer. Chromogenic reagents A and B were added sequentially, followed by gentle shaking and further incubation at 37°C in the dark for 15 min to develop color. The reaction was halted by adding 50 μL of stop solution, and the optical density (OD) was measured at 450 nm.

Immunofluorescence (IFC) staining was used to visualize the expressions of NGF, TNF-α, IFN-γ, IL-4, and IL-10 in nasal mucosal tissue samples. Tissue sections were first baked in a 65°C oven for 2 h, then treated with xylene for 10 min, followed by a second xylene treatment for another 10 min. The sections were then sequentially immersed in 100%, 95%, and 80% ethanol, followed by purified water, each for 5 min. After antigen retrieval, sections were rinsed with PBS. To permeabilize the tissue, 0.5% Triton X-100 solution was applied at room temperature for 20 min. The sections were then washed three times with PBS. To block non-specific binding, 5% bovine serum albumin was added and incubated at 37°C for 30 min. After returning the sections to room temperature, they were washed with PBS three times, each for 3 min. Excess liquid was removed with absorbent paper. Primary antibody (Abcam, USA), diluted 1:100, was added and incubated overnight at 4°C in a humid chamber. After incubation, the sections were brought back to room temperature, washed three times with PBS, and excess liquid was removed. Fluorescent secondary antibody (Beijing Zhongshan Jinqiao Biotechnology Co., Ltd., China), diluted 1:200, was applied and incubated at 37°C for 30 min in a humid chamber. The sections were then stained with 4′,6-diamidino-2-phenylindole (DAPI, Jiangsu Ketai Biological Technology Co., Ltd., China) in the dark for 5 min to highlight the nuclei. Excess DAPI was removed with PBS, followed by a quick rinse with tap water. The sections were mounted with anti-fluorescence quenching medium and examined under a microscope (Olympus Corporation, Japan). IFC was used to detect the expression of NGF, TNF-α, IFN-γ, IL-4, and IL-10. Paraffin-embedded tissue sections with a thickness of 5 μm were prepared. The slides were deparaffinized, rehydrated, subjected to antigen retrieval, and then stained for IFC.

Statistical Analysis

The statistical analysis of the collected data was conducted using Statistical Package for the Social Sciences (SPSS) software version 22.0 (IBM Corp., Armonk, NY, USA). The primary objective of the analysis was to determine the significance of the differences observed between the control group, modeling group, and model control group.

Descriptive Statistics

The data are presented as mean ± standard deviation. The mean provides an average value for each group, while the standard deviation measures the dispersion or variability around this mean. This approach allows for a clear understanding of the central tendency and variability within each group.

Comparative Analysis

To compare the means among multiple groups, a one-way analysis of variance (ANOVA) was performed. ANOVA is a statistical test used to determine if there are any statistically significant differences between the means of three or more independent groups. In this study, ANOVA was employed to assess the overall effect of the different treatments on the measured outcomes, such as NGF levels, cytokine concentrations, and AR symptom scores. ANOVA was used to assess the significant effects of factors A, B, C, and D on the experimental outcome (chlorogenic acid content). The sum of squares, mean square, F-value, and degrees of freedom for each factor were calculated. If the F-value exceeded the critical value (determined by the significance level α and degrees of freedom), the factor was considered to have a significant effect on the experimental outcome.

Post Hoc Testing

If ANOVA indicated significant differences among groups, *post hoc* pairwise comparisons were carried out to identify which specific groups differed from each other. The least significant difference test was utilized for these comparisons. The least significant difference test is a type of *post hoc* test that helps to determine which pairs of groups have significant

differences, while controlling the type I error rate. It is considered a straightforward and relatively liberal test for pairwise comparisons when the overall ANOVA is significant. The *F*-value is a statistic calculated using ANOVA, which is used to determine whether the effects of various factors on the experimental results are significant. The calculation equation is as follows:

$$F = \frac{MS_{\text{factor}}}{MS_{\text{error}}}$$

Data Interpretation

The results from these statistical tests were interpreted to draw conclusions about the efficacy of the treatments and the biological implications of the findings. Statistically significant results were used to determine the impact of the interventions on AR symptoms and molecular markers, guiding further analysis and potential therapeutic implications.

Significance Level

The threshold for statistical significance was set at a *p* value of less than .05. This means that any *p* value below .05 was considered evidence of a statistically significant difference between groups. The *p* value represents the probability that the observed differences occurred by chance. A *p* value lower than .05 indicates that the likelihood of the differences being due to random variation alone is less than 5%, thereby supporting the rejection of the null hypothesis that assumes no effect or difference.

Results

HPLC Analysis

HPLC analysis provided crucial insights into the successful extraction of chlorogenic acid from LJE. The chromatographic profiles obtained for LJE were compared against the standard chlorogenic acid chromatogram, and the results demonstrated a significant overlap. The retention time of chlorogenic acid in the LJE chromatogram was observed to be approximately 15 min, aligning well with the standard. This clear correlation confirms that chlorogenic acid was effectively extracted from the LJE, validating the extraction process and ensuring the presence of the target compound. Figure 1 illustrates this alignment, showcasing the HPLC chromatograms for both the LJE and the chlorogenic acid reference standard.

Orthogonal Experiment Results

The orthogonal experiment aimed to identify the most influential factors affecting the yield of chlorogenic acid extraction. The results, detailed in Table 3, revealed that ethanol concentration was the most critical factor impacting the extraction efficiency. This was followed by the pH level, with extraction time and solvent-to-material ratio showing comparatively smaller effects. The variance analysis, as presented in Table 4, confirmed that ethanol concentration had the highest impact on the extraction rate, with a significant *F*-value of 4.725 and a *p* value of .31. This finding underscores the dominance of ethanol concentration in determining the extraction yield, while the other factors did not demonstrate significant statistical effects.

A larger *R*-value indicates a more significant effect of the factor on the result, while a smaller *R*-value suggests a lesser impact of the factor on the result.

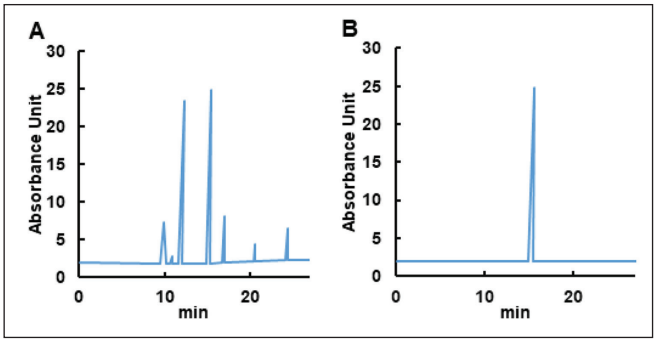


Figure 1. High-performance Liquid Chromatography (HPLC) Chromatograms Comparing *Lonicera japonica* Extract (LJE) with Chlorogenic Acid Standard, Highlighting the Successful Extraction of Chlorogenic Acid.

Single-factor Analysis Results

Building on the orthogonal experiment, single-factor analysis was employed to refine the extraction conditions. The single-factor analysis results, depicted in Figure 2, demonstrated that increasing the ethanol concentration led to higher chlorogenic acid yields, peaking at a concentration of 70%. Beyond this concentration, the yield slightly decreased, suggesting a saturation point. Similarly, the pH level also influenced the extraction yield, with the highest efficiency observed at pH 5. Both ethanol concentration and pH were identified as the primary factors affecting the extraction process. Based on these findings, the optimal extraction conditions were determined to be a 70% ethanol solution with a pH of 5. For practical purposes, a solvent-to-material ratio of 10 times and an extraction time of 1.5 h were selected to maximize efficiency while maintaining simplicity.

AR Symptom Scores

The evaluation of AR symptoms in mice provided valuable insights into the effectiveness of the treatments. The AR symptom scores of the three treatment groups after 2 weeks were statistically analyzed, and the results comparing pre-treatment and post-treatment are shown in Figure 3. Mice in the control group, which received no intervention, exhibited

Table 3. Summary of the Orthogonal Experiment Showing the Effects of Ethanol Concentration, Extraction Time, Solvent-to-material Ratio, and pH on Chlorogenic Acid Yield.

Sequence	Ethanol Concentration (%, A)	Extraction Time (h, B)	Solvent-to-material Ratio (Times, C)	pH (D)	Chlorogenic Acid (mg g^{-1})
1	1	1	1	1	9.114
2	1	2	2	2	13.498
3	1	3	3	3	11.001
4	1	4	4	4	9.02
5	2	2	1	3	12.947
6	2	1	2	4	13.518
7	2	4	3	1	11.294
8	2	3	4	2	17.157
9	3	3	1	4	13.205
10	3	4	2	3	15.022
11	3	1	3	2	12.884
12	3	2	4	1	11.587
13	4	4	1	2	14.044
14	4	3	2	1	13.653
15	4	2	3	4	15.977
16	4	1	4	3	14.284
K1	9.947	12.585	12.389	11.307	
K2	14.082	13.739	13.704	15.133	
K3	13.496	13.926	13.081	12.982	
K4	14.593	11.909	13.396	12.593	
R	4.034	0.994	0.115	3.527	

Note: K1, K2, K3, and K4 represent the mean effects of different levels of each factor (ethanol concentration, extraction time, solvent volume, pH) on the experimental outcome (i.e., chlorogenic acid content). R represents the range, calculated as R = max (K1, K2, K3, K4) – min (K1, K2, K3, K4). It reflects the significance of the impact of different levels on the experimental outcome.

Table 4. Variance Analysis Results Illustrate the Impact of Different Factors on Chlorogenic Acid Extraction Efficiency.

Factor	Sum of Squares	Degree of Freedom	Mean Square Error	*F*	*p*
A	53.024	3	11.937	4.725	.31
B	17.329	3	0.181	0.04	
C	6.903	3	4.736	0.925	
D	30.082	3	9.486	3.971	

Note: A: ethanol concentration; B: extraction time; C: solvent-to-material ratio; D: pH value. A larger *F*-value indicates a more significant effect of the corresponding factor on the experimental results.

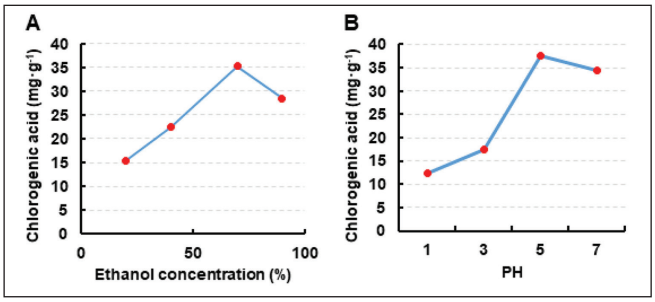


Figure 2. Single-factor Analysis Results Showing the Effect of Ethanol Concentration and pH on Chlorogenic Acid Extraction Efficiency.

stable symptom scores before and after the treatment period, indicating no significant changes ($p > .05$). In contrast, the modeling group and model control group, which underwent different treatment regimens, showed markedly higher symptom scores before treatment, recorded as 8.11 ± 0.51 and 8.08 ± 0.48, respectively. These scores were significantly elevated compared to the control group ($p < .05$), highlighting the presence of AR symptoms. After administering the treatment, the symptom scores in the modeling group showed a significant reduction and approached levels similar to those of the control group ($p < .05$). This indicates that the treatment effectively alleviated AR symptoms. Conversely, the model control group, which received saline instead of LJE,

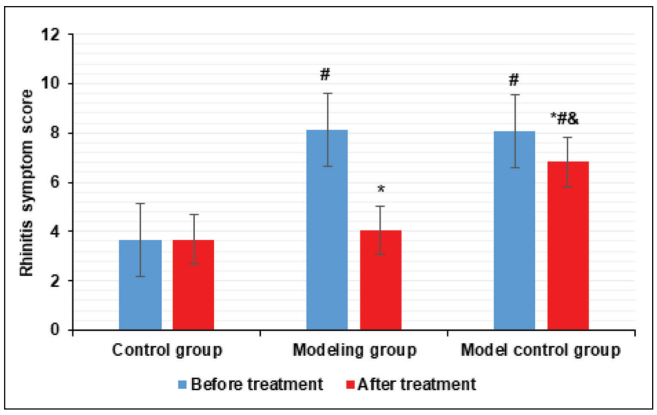


Figure 3. Graphical Representation of Allergic Rhinitis (AR) Symptom Scores Before and After Treatment, Showing Differences Among the Control Group, Modeling Group, and Model Control Group.

Note: *Compared with pre-treatment values, $p < .05$; #compared with control group, $p < .05$; and compared with modeling group, $p < .05$.

continued to exhibit higher symptom scores compared to the modeling group ($p < .05$), as illustrated in Figure 3.

Detection Results of PI3K/AKT Signaling Pathway-related Proteins

The assessment of PI3K and AKT proteins in nasal mucosal tissues revealed specific trends across the three groups: control group, modeling group, and model control group. In the modeling group, both PI3K and AKT levels were slightly elevated compared to the control group, although this increase was not statistically significant ($p > .05$). This suggests that while there is a noticeable trend toward higher protein levels, the difference is not substantial enough to be considered significant in the context of the study.

In contrast, the model control group demonstrated a pronounced upregulation of PI3K and AKT, with the highest observed levels among all the groups. This significant elevation was statistically significant ($p < .05$), indicating a robust activation of these signaling pathways in the model control group. Such findings suggest that the intervention in the model control group strongly influences the PI3K/AKT signaling pathway, which is crucial for various cellular processes. Figure 4 visually represents these findings, with Panels A and B showing the quantitative analysis of the protein levels, and Panel C presenting the Western blot analysis results for a clear depiction of the protein expression patterns.

Figure 4 provides a graphical representation of the PI3K and AKT protein levels across different groups, namely, control group, modeling group, and model control group. Panels A and B display the quantitative data, showing how the levels of these proteins vary among the groups. Panel C illustrates the Western blot analysis results, highlighting the differences in protein expression.

Detection Results of NF-κB Signaling Pathway-related Proteins

The assessment of NF-κB p65 protein levels in the nasal mucosa tissue revealed that the modeling group exhibited a marginal increase in NF-κB p65 compared to the control group, but this difference was not statistically significant ($p > .05$). This indicates that the treatment had a minor effect on NF-κB p65 expression in the modeling group. However, the model control group showed a significant increase in NF-κB p65 levels, which were notably higher compared to both the control group and modeling group ($p < .05$). This substantial elevation suggests a pronounced activation of NF-κB signaling in the model control group, which is a critical pathway involved in inflammatory responses. Figure 5 illustrates these results, with Panel A showing the quantitative analysis of NF-κB p65 levels and Panel B providing the Western blot analysis results that visualize the differences in protein expression. Figure 5 exhibits the changes in NF-κB p65 protein levels across the control group, modeling group, and model control group. Panel A shows the quantitative data, indicating variations in NF-κB p65 levels. Panel B presents the Western blot analysis, offering a visual representation of the protein expression.

Detection Results of NGF

The evaluation of NGF levels showed that the modeling group had slightly higher NGF levels compared to the control group, but this difference was not statistically significant ($p > .05$). This suggests that while there is a trend toward increased NGF expression, it is not substantial enough to be deemed significant. In the model control group, however, NGF levels were significantly elevated compared to both the control group and modeling group ($p < .05$). This indicates a strong upregulation of NGF in response to the treatment. IFC staining further confirmed these findings, revealing a marked increase in NGF-positive spots in the nasal mucosa tissue of the model control group. Figure 6 details these results, with Panel A displaying serum NGF levels and Panel B showing the IFC staining results for NGF in nasal mucosa tissue. Figure 6 shows the NGF levels across the control group, modeling group, and model control group. Panel A presents the NGF concentrations in serum, while Panel B illustrates the IFC staining results of NGF in nasal mucosa tissue (×100 magnification). Statistical significance is indicated with # for comparisons to the control group ($p < .05$) and for comparisons to the modeling group ($p < .05$).

Detection Results of Pro-inflammatory Factors

The analysis of pro-inflammatory factors, including TNF-α and IFN-γ, revealed that the modeling group had higher levels of these cytokines compared to the control group, though the difference was not statistically significant ($p > .05$). This

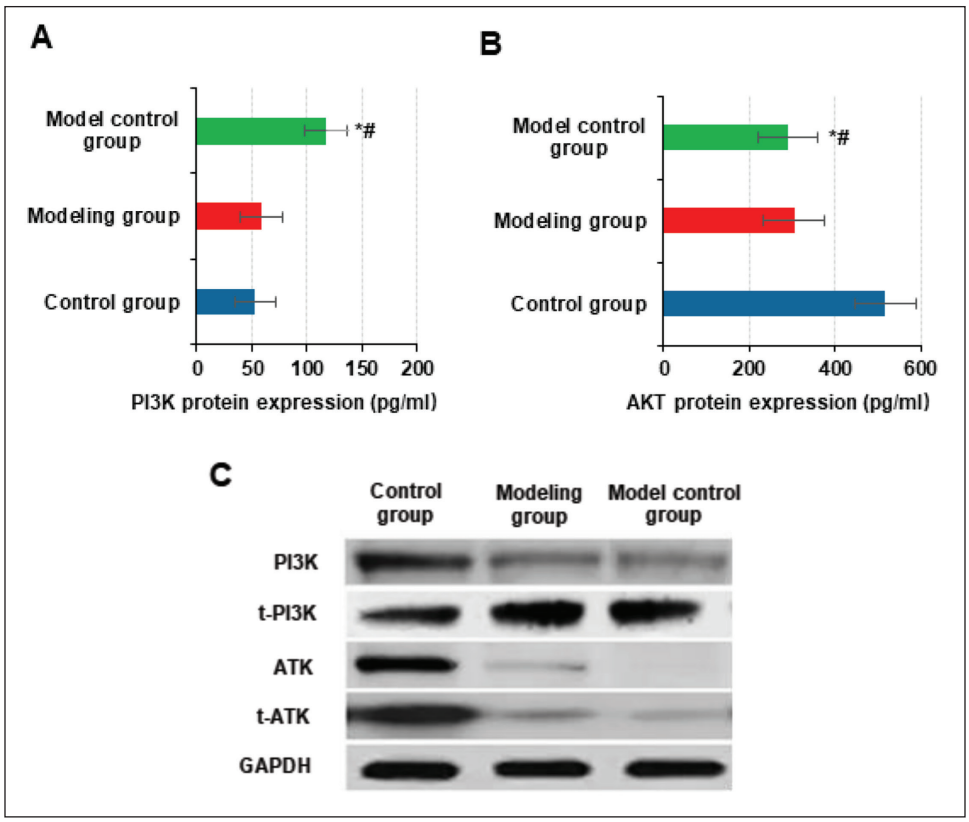


Figure 4. Expression Levels of PI3K/AKT Signaling Pathway Proteins. (A) Quantitative Assessment of PI3K Levels Across Control Group, Modeling Group, and Model Control Group; (B) Quantitative Assessment of AKT Levels Across Control Group, Modeling Group, and Model Control Group; and (C) Western Blot Analysis Displaying Protein Bands for PI3K and AKT.

Note: #Compared with control group, $p < .05$; and compared with modeling group, $p < .05$.

suggests a trend toward increased pro-inflammatory activity in the modeling group, but it does not reach statistical significance. In contrast, the model control group exhibited the highest levels of TNF-α and IFN-γ among all groups, with statistically significant differences ($p < .05$) compared to both the control group and the modeling group. This significant elevation indicates a robust inflammatory response in the model control group. IFC staining also revealed a greater number of positive spots for TNF-α and IFN-γ in the nasal mucosa tissue of the model control group, further corroborating the increased inflammatory activity. Figure 7 provides a comprehensive view of these results, with Panels A and B showing serum levels of TNF-α and IFN-γ, and Panels C and D displaying the IFC staining results. Figure 7 depicts the levels of pro-inflammatory factors across the control group, modeling group, and model control group. Panels A and B illustrate serum concentrations of TNF-α and IFN-γ, while Panels C and D present the IFC staining results for these factors in nasal mucosa tissue. Statistical comparisons are marked with # for differences compared to the control group ($p < .05$) and for differences compared to the modeling group ($p < .05$).

Detection Results of Anti-inflammatory Factors

The results for anti-inflammatory factors IL-4 and IL-10 showed that levels in the modeling group were somewhat lower compared to the control group, but this difference was not statistically significant ($p > .05$). This suggests that while there may be a trend toward lower anti-inflammatory activity in the modeling group, it does not reach statistical significance. In contrast, the model control group showed significantly higher levels of IL-4 and IL-10 compared to the other groups ($p < .05$). This indicates a notable anti-inflammatory response in the model control group. IFC staining revealed fewer positive spots for IL-4 and IL-10 in the nasal mucosa tissue of the model control group, suggesting a more complex pattern of anti-inflammatory activity. Figure 8 details these findings, with Panels A and B showing serum levels of IL-4 and IL-10, and Panels C and D presenting the IFC staining results. Figure 8 provides an overview of anti-inflammatory factor levels across the control group, modeling group, and model control group. Panels A and B show serum concentrations of IL-4 and IL-10, while Panels C and D illustrate the IFC staining results for these factors in nasal mucosa tissue.

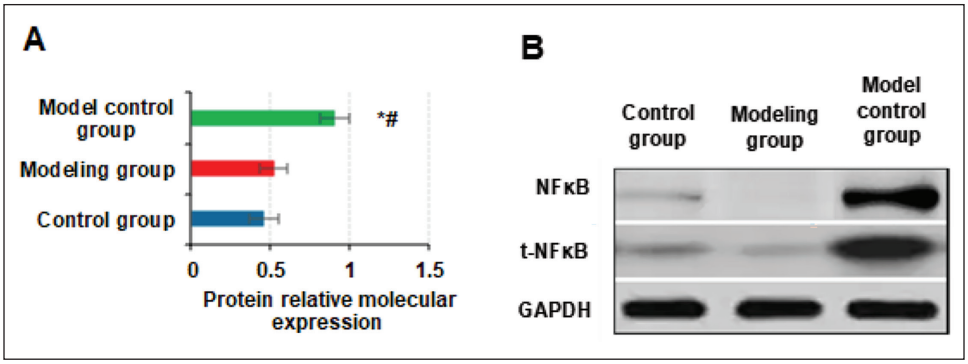


Figure 5. NF-κB Pathway Protein Expression Changes. (A) Quantitative Measurement of NF-κB p65 Levels in Control Group, Modeling Group, and Model Control Group; (B) Western Blot Results Showing NF-κB p65 Protein Bands.

Note: #Compared with control group, $p < .05$; and compared with modeling group, $p < .05$.

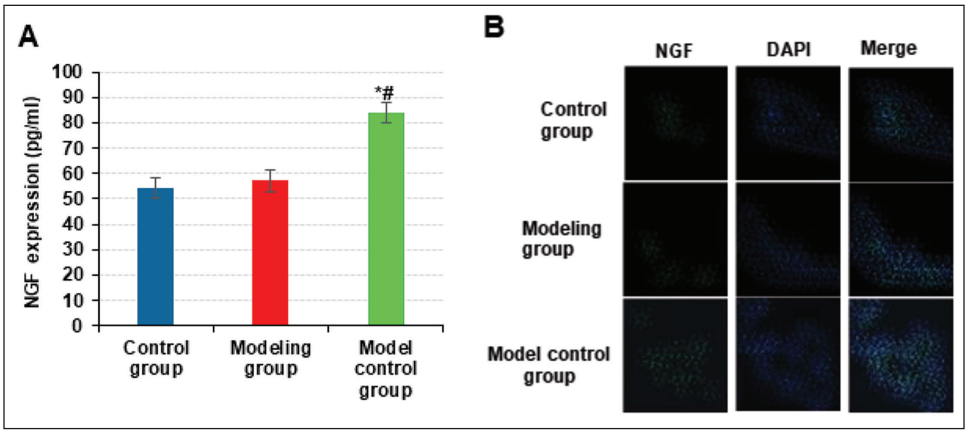


Figure 6. Nerve Growth Factor (NGF) Levels in Various Groups. (A) Serum NGF Concentrations Across Different Control Group, Modeling Group, and Model Control Group and (B) Immunofluorescence Staining Showing NGF-positive Spots in Nasal Mucosa Tissue (×100).

Note: #Compared with control group ($p < .05$); and compared with modeling group ($p < .05$).

Discussion

The findings from this study provide valuable insights into optimizing the extraction process of chlorogenic acid from LJE and its therapeutic potential in treating AR. This discussion will delve into the implications of the optimal extraction conditions identified, the efficacy of LJE in AR treatment, and the role of specific signaling pathways and inflammatory factors.

Optimal Extraction Conditions for Chlorogenic Acid

The research determined that the most effective conditions for extracting chlorogenic acid from *L. japonica* using ethanol reflux were a 70% ethanol concentration, a pH of 5, a solvent-to-material ratio of 10 times the amount of herbal material, and an extraction time of 1.5 h. These conditions were derived from evaluating various factors affecting the extraction process. The choice of 70% ethanol aligns with previous studies that highlight its effectiveness in dissolving a wide range of phytochemicals, including chlorogenic acid, while minimizing the co-extraction of unwanted compounds. The pH of 5 was found to be optimal, as it maintains the stability of chlorogenic acid and maximizes its solubility in the ethanol-water mixture.

Despite the promising results, the study focused solely on ethanol reflux extraction. Future research could broaden the scope by comparing ethanol reflux with alternative methods such as ultrasound-assisted extraction or water extraction (Pimpley et al., 2020; Saleh et al., 2016). These methods might offer different efficiencies or benefits. Additionally, factors like extraction temperature and the liquid-to-material ratio could also influence the yield of chlorogenic acid (Frosi et al., 2021; Yu et al., 2019). Exploring these variables could refine the extraction

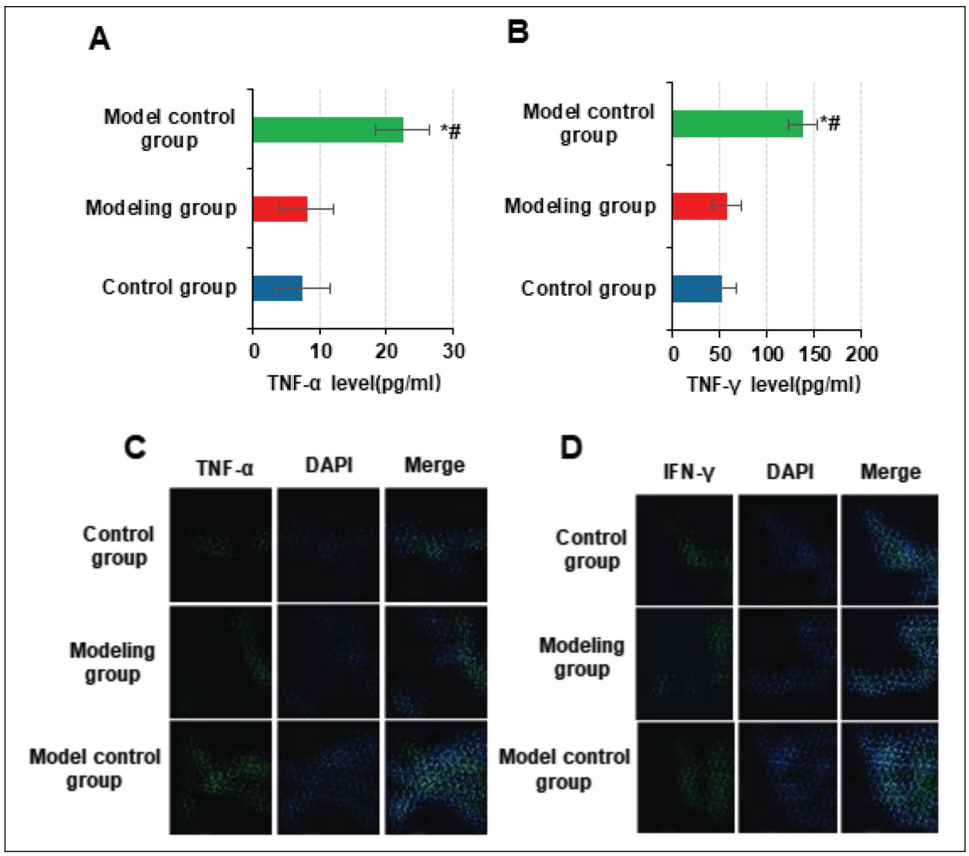


Figure 7. Levels of Pro-inflammatory Factors. (A) Serum Levels of Tumor Necrosis Factor (TNF)-α Across Control Group, Modeling Group, and Model Control Group; (B) Serum Levels of Interferon (IFN)-γ Across Control Group, Modeling Group, and Model Control Group; (C) Immunofluorescence Staining Revealing TNF-α Positive Spots in Nasal Mucosa Tissue (×100); (D) Immunofluorescence Staining Revealing IFN-γ Positive Spots in Nasal Mucosa Tissue (×100).

Note: #Compared with control group ($p < .05$); and compared with modeling group ($p < .05$).

process further, enhancing the efficiency and yield of chlorogenic acid from *L. japonica*.

Efficacy of LJE in Treating AR

The evaluation of AR symptoms in mice serves as a critical measure of the therapeutic efficacy of LJE. Before treatment, both the modeling group and model control group showed elevated symptom scores, indicating successful modeling establishment for AR. This aligns with established research demonstrating similar symptom scores in the AR model (Chen et al., 2022; Cheng et al., 2020). After treatment, the modeling group exhibited a significant reduction in symptom scores, approaching those of the control group, indicating that LJE effectively alleviated nasal inflammation and other AR symptoms. The model control group, however, continued to show higher scores, suggesting that while LJE has therapeutic potential, its efficacy might vary under different conditions or dosages. The reduction in symptom scores observed in the modeling group highlights LJE's anti-inflammatory properties. This finding is consistent with the role of anti-inflammatory agents in managing AR, which often involves reducing nasal inflammation and associated symptoms. The results underscore the potential of LJE as a valuable treatment option for AR, providing a basis for further investigation into its mechanisms and efficacy.

PI3K/AKT and NF-κB Signaling Pathways

The activation of the PI3K/AKT signaling pathway in the model control group, as evidenced by elevated levels of PI3K and AKT, suggests its involvement in the inflammatory response of the AR modeling. This pathway plays a crucial role in regulating cellular processes such as growth, survival, and metabolism (Tewari et al., 2022). Previous studies have linked the PI3K/AKT pathway to various inflammatory and immune responses, including rhinitis (Wang et al., 2024; Yuan et al., 2022; Zeng et al., 2020). The significant down-regulation of PI3K and AKT in the modeling group, following LJE treatment, indicates that LJE might exert its effects

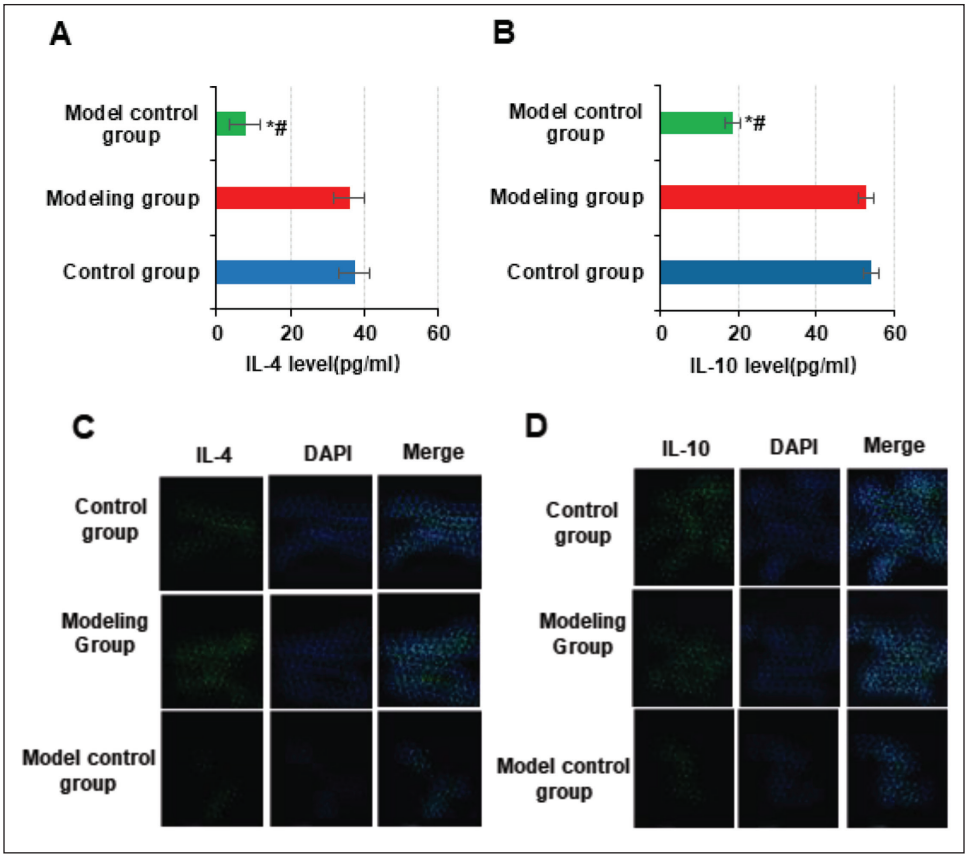


Figure 8. Anti-inflammatory Factor Levels in Serum and Tissues. (A) Serum Concentrations of Interleukin (IL)-4 Across Different Groups; (B) Serum Concentrations of IL-10 Across Different Groups; (C) Immunofluorescence Staining Showing IL-4 Positive Spots in Nasal Mucosa Tissue (×100); (D) Immunofluorescence Staining Showing IL-10 Positive Spots in Nasal Mucosa Tissue (×100).

Note: #Compared with control group ($p < .05$); and compared with modeling group ($p < .05$).

by inhibiting this pathway, thereby reducing inflammation and improving AR symptoms.

Similarly, the NF-κB signaling pathway, particularly the NF-κB p65 subunit, is known for its role in regulating immune and inflammatory responses (Ren et al., 2020; Yu et al., 2020). The pronounced increase in NF-κB p65 levels in the model control group suggests activation of this pathway, correlating with heightened inflammatory responses. The fact that NF-κB p65 levels in the modeling group were similar to those in the control group, following LJE treatment, implies that LJE may regulate the NF-κB pathway, mitigating its activation and consequently reducing inflammation. This observation supports the hypothesis that LJE's therapeutic effects might involve inhibition of the NF-κB pathway, contributing to its anti-inflammatory properties (Piao et al., 2020, 2021; Tian et al., 2023).

NGF Levels

NGF is essential for the survival, growth, and differentiation of nerve cells. Increased NGF levels have been associated with inflammatory conditions, including AR (Klimek et al., 2023; Sacchetti et al., 2019). The significantly higher NGF levels in the model control group suggest an enhanced inflammatory response in the nasal mucosa. LJE treatment led to a notable reduction in NGF levels in the modeling group, indicating that LJE might alleviate inflammation by regulating NGF expression. This finding aligns with the observed therapeutic effects of LJE, suggesting that NGF regulation could be one of the mechanisms through which LJE exerts its anti-inflammatory effects.

Pro-inflammatory Factors

The elevated levels of pro-inflammatory cytokines such as TNF-α and IFN-γ in the model control group further corroborate the increased inflammatory response in AR (Oh et al., 2022). These cytokines are known to activate immune cells and promote inflammation. The significant reduction of TNF-α and IFN-γ in the modeling group, following LJE treatment, supports the idea that LJE possesses anti-inflammatory properties by suppressing the production of these cytokines.

This finding highlights the potential of LJE in managing inflammation associated with AR.

Anti-inflammatory Factors

IL-4 and IL-10 are crucial in regulating and mitigating inflammation. They help restore tissue balance and counteract inflammation-induced damage (Moulik et al., 2021). The observed decrease in IL-4 and IL-10 levels in the model control group could be attributed to the heightened inflammatory response. However, LJE treatment in the modeling group potentially elevated IL-4 and IL-10 levels, suggesting that LJE might not only suppress pro-inflammatory factors but also enhance anti-inflammatory responses. This dual effect could contribute to the overall anti-inflammatory action of LJE in treating AR. This study successfully identified optimal conditions for extracting chlorogenic acid from *L. japonica* using ethanol reflux and demonstrated the therapeutic potential of LJE in treating AR. The results suggest that LJE may exert its anti-inflammatory effects through the regulation of key signaling pathways such as PI3K/AKT and NF-κB, as well as by influencing levels of NGF and inflammatory cytokines. Further research exploring additional extraction methods and a broader range of influencing factors could provide deeper insights into optimizing chlorogenic acid extraction and enhancing the therapeutic efficacy of LJE.

Pharmacological Effects of LJE

LJE contains a variety of bioactive compounds, including chlorogenic acid, luteolin, quercetin, and other flavonoids, as well as essential oils. These components endow LJE with diverse pharmacological activities. From an anti-inflammatory perspective, LJE is capable of inhibiting the release of various inflammatory mediators. Chlorogenic acid can reduce the production of pro-inflammatory cytokines, such as TNF-α and IL-6, by suppressing the NF-κB signaling pathway, thereby alleviating the inflammatory response. In this study, LJE may act on the AR mouse model through similar anti-inflammatory mechanisms to reduce the degree of nasal mucosal inflammation. In terms of immune modulation, LJE exerts a biphasic effect on the immune system. On one hand, it enhances the body's innate immune functions, such as promoting macrophage phagocytosis and increasing non-specific immune defense. On the other hand, it can regulate abnormal immune responses. In AR, LJE may correct the Th2 cell-dominant immune imbalance by modulating the Th1/Th2 cell balance. Research showed that water-extracted honeysuckle polysaccharides improve AR by repairing the intestinal barrier and inhibiting NLRP3 inflammasome-driven inflammation and Th17 immune responses (Bai et al., 2022). Li et al. (2022) reported that *Laggera retrofracta* herb (LRH)-type flavonoids exhibit multifaceted protective effects on dextran sulfate sodium (DSS)-induced colitis in mice by alleviating colonic inflammation and oxidative stress, restoring epithelial barrier function, and possibly improving the intestinal microenvironment through the modulation of the PI3K/AKT pathway. Han et al. (2016) indicated that LJE suppresses TNF-α and IL-1β-induced inflammation in BV2 microglial cells through the PI3K/Akt/NF-κB signaling pathway. Kwon et al. (2012) found that LJE has potent neuroprotective effects against Parkinson's disease, which are at least partially mediated through the activation of MAPK, PI3K/Akt, and NF-κB pathways to inhibit neurotoxicity, apoptotic cascades, and oxidative stress. Li et al. demonstrated that LJE alleviates ovalbumin-induced AR by inhibiting AR-induced inflammation and autoimmunity. Furthermore, LJE exhibits antioxidant activity. The flavonoids and phenolic acids it contains are effective antioxidants that can scavenge excessive reactive oxygen species and free radicals in the body, reducing oxidative stress-induced cellular damage. In AR, oxidative stress can lead to epithelial cell damage in the nasal mucosa, increased infiltration of inflammatory cells, and exacerbation of the condition. The antioxidant effects of LJE help mitigate oxidative damage to the nasal mucosa, thereby maintaining its normal physiological function.

This study found that LJE significantly reduced the expression levels of NGF in both nasal mucosal tissues and serum in an AR mouse model. Based on the pharmacological properties of LJE, it is speculated that its regulatory effects may be mediated through the following mechanisms. Due to its anti-inflammatory and immunomodulatory actions, LJE can alleviate inflammation in the nasal mucosa and reduce the infiltration of inflammatory cells. Inflammatory cells, such as eosinophils and mast cells, upon activation, release various cytokines and mediators that stimulate the synthesis and release of NGF. By inhibiting the activation of inflammatory cells and the release of inflammatory mediators, LJE reduces the stimulation of NGF expression and lowers NGF levels. From a neuroprotective and repair perspective, the antioxidant properties of LJE can mitigate oxidative stress-induced damage to nerve fibers. In AR, oxidative stress may cause nerve fiber damage, leading to neurogenic inflammation and increased NGF expression. LJE, through its antioxidant effects, protects nerve fibers, reduces neural injury, and indirectly inhibits the overexpression of NGF.

Additionally, LJE may directly act on nasal mucosal cells, modulating signaling pathways associated with NGF expression. Although the specific signaling pathways have not been fully elucidated, previous studies have suggested that certain components of LJE can influence the activity of intracellular protein kinases and transcription factors, thereby regulating gene expression. In this study, LJE may regulate the relevant signaling pathways, suppressing the transcription and translation of the NGF gene, thereby reducing NGF synthesis and release. One limitation of this study is the small sample size, which warrants the need for larger-scale, multicenter clinical studies in future research.

Conclusion

In summary, LJE significantly reduced the expression of NGF in an AR model and alleviated rhinitis symptoms. LJE is likely to exert its anti-inflammatory effects through the modulation of the PI3K/AKT and NF-κB signaling pathways. Future research could further increase the sample size and conduct more in-depth molecular mechanism studies to explore the relationship between LJE and signaling pathways, as well as its impact on other immunomodulatory factors.

Abbreviations

ANOVA: Analysis of variance; AR: Allergic rhinitis; DAPI: 4′,6-Diamidino-2-phenylindole; ELISA: Enzyme-linked immunosorbent assays; HPLC: High-performance liquid chromatography; LJE: *Lonicera japonica* extract; NGF: Nerve growth factor; OD: Optical density; PBS: Phosphate buffered solution.

Authors Contribution

Conception and study design: Zhifeng Deng and Minli Zhang; data acquisition and analysis: Ting Zhu, Xiaoting Tong, Wendan Shi, and Yu Xu; manuscript draft, editing, and revision: Zhifeng Deng and Minli Zhang. All authors wrote and approved the final manuscript.

Availability of Data and Material

All data generated during this study are included in this published article.

Declaration of Conflicting Interests

The authors declared no potential conflicts of interest with respect to the research, authorship, and/or publication of this article.

Ethical Approval

All animal experiments were approved by the Animal Ethics Committee of Renmin Hospital of Wuhan University, in compliance with Chinese national guidelines for the care and use of animals.

Funding

The authors received no financial support for the research, authorship, and/or publication of this article.

Informed Consent

Not applicable.

ORCID iD

Minli Zhang https://orcid.org/0009-0005-8197-7773

References

Bai, X., Liu, P., Shen, H., Zhang, Q., Zhang, T., & Jin, X. (2022). Water-extracted *Lonicera japonica* polysaccharide attenuates allergic rhinitis by regulating NLRP3-IL-17 signaling axis. *Carbohydrate Polymers*, 297, Article 120053. https://doi.org/10.1016/j.carbpol.2022.120053

Bousquet, J., Anto, J. M., Bachert, C., Baiardini, I., Bosnic-Anticevich, S., Walter Canonica, G., Melén, E., Palomares, O., Scadding, G. K., Togias, A., & Toppila-Salmi, S. (2020). Allergic rhinitis. *Nature Reviews Disease Primers*, *6*(1), 95. https://doi.org/10.1038/s41572-020-00227-0

Chen, H., Cheng, Y., Du, H., Zhang, C., Zhou, Y., Zhao, Z., Li, Y., Friedemann, T., Mei, J., Schröder, S., & Chen, M. (2022). Shufeng Jiedu capsule ameliorates olfactory dysfunction via the AMPK/mTOR autophagy pathway in a mouse model of allergic rhinitis. *Phytomedicine*, 107, Article 154426. https://doi.org/10.1016/j.phymed.2022.154426

Cheng, F.-L., An, Y.-F., Han, Z.-Q., Li, C., Li, Z.-Q., Yang, P.-C., & Zhao, C.-Q. (2020). Period2 gene regulates diurnal changes of nasal symptoms in an allergic rhinitis mouse model. *International Forum of Allergy and Rhinology*, *10*(11), 1236–1248. https://doi.org/10.1002/alr.22607

Du, X.-Q., Shi, L.-P., Cao, W.-F., Chen, Z.-W., Zuo, B., & Hu, J.-Y. (2021). Add-on effect of honeysuckle in the treatment of coronavirus disease 2019: A systematic review and meta-analysis. *Frontiers in Pharmacology*, 12, Article 708636. https://doi.org/10.3389/fphar.2021.708636

Frosi, I., Montagna, I., Colombo, R., Milanese, C., & Papetti, A. (2021). Recovery of chlorogenic acids from agri-food wastes: Updates on green extraction techniques. *Molecules*, *26*(15), 4515. https://doi.org/10.3390/molecules26154515

Gołba, M., Sokół-Łętowska, A., & Kucharska, A. Z. (2020). Health properties and composition of honeysuckle berry *Lonicera caerulea* L. an update on recent studies. *Molecules*, *25*(3), 749. https://doi.org/10.3390/molecules25030749

Golubev, D., Zemskaya, N., Shevchenko, O., Shaposhnikov, M., Kukuman, D., Patov, S., Punegov, V., & Moskalev, A. (2022). Honeysuckle extract (*Lonicera pallasii* L.) exerts antioxidant properties and extends the lifespan and healthspan of *Drosophila melanogaster*. *Biogerontology*, *23*(2), 215–235. https://doi.org/10.1007/s10522-022-09954-1

Guo, L., Qiao, J., Zhang, L., Yan, W., Zhang, M., Lu, Y., Wang, Y., Ma, H., Liu, Y., Zhang, Y., Li, J., Qin, D., & Huo, J. (2023). Critical review on anthocyanins in blue honeysuckle (*Lonicera caerulea* L.) and their function. *Plant Physiology and Biochemistry*, 204, Article 108090. https://doi.org/10.1016/j.plaphy.2023.108090

Han, M. H., Lee, W. S., Nagappan, A., Hong, S. H., Jung, J. H., Park, C., Kim, H. J., Kim, G.-Y., Kim, G., Jung, J.-M., Ryu, C. H., Shin, S. C., Hong, S. C., & Choi, Y. H. (2016). Flavonoids isolated from flowers of *Lonicera japonica* Thunb. inhibit inflammatory responses in BV2 microglial cells by suppressing TNF-α and IL-β through PI3K/Akt/NF-kb signaling pathways. *Phytotherapy Research*, *30*(11), 1824–1832. https://doi.org/10.1002/ptr.5688

Klimek, L., Werminghaus, P., Bergmann, C., Hagemann, J., Huppertz, T., Bärhold, F., Klimek, F., Dziadziulia, K., Casper, I., Polk, M. L., Cuevas, M., Gröger, M., & Becker, S. (2023). Neuroimmunology of allergic rhinitis: Part 1: Cellular and humoral basic principles. *HNO*, *71*(5), 337–346. https://doi.org/10.1007/s00106-023-01292-z

Kweon, B., Oh, J., Lim, Y., Noh, G., Yu, J., Kim, D., Jang, M., Kim, D., & Bae, G. (2024, November 19). Anti-inflammatory effects

of honeysuckle leaf against lipopolysaccharide-induced neuroinflammation on BV2 microglia. *Nutrients*, *16*(22), 3954. https://doi.org/10.3390/nu16223954

Kwon, S.-H., Hong, S.-I., Jung, Y.-H., Kim, M.-J., Kim, S.-Y., Kim, H.-C., Lee, S.-Y., & Jang, C.-G. (2012). *Lonicera japonica* THUNB. protects 6-hydroxydopamine-induced neurotoxicity by inhibiting activation of MAPKs, PI3K/Akt, and NF-κB in SH-SY5Y cells. *Food and Chemical Toxicology*, *50*(3–4), 797–807. https://doi.org/10.1016/j.fct.2011.12.026

Li, S., Jia, K., Wen, Y., Liu, T., & Tao, D. (2021). Orthogonal deep neural networks. *IEEE Transactions on Pattern Analysis and Machine Intelligence*, *43*(4), 1352–1368. https://doi.org/10.1109/TPAMI.2019.2948352

Li, C., Wang, L., Zhao, J., Wei, Y., Zhai, S., Tan, M., Guan, K., Huang, Z., & Chen, C. (2022). *Lonicera rupicola* Hook.f.et Thoms flavonoids ameliorated dysregulated inflammatory responses, intestinal barrier, and gut microbiome in ulcerative colitis via PI3K/AKT pathway. *Phytomedicine*, 104, Article 154284. https://doi.org/10.1016/j.phymed.2022.154284

Liang, C., Hui, N., Liu, Y., Qiao, G., Li, J., Tian, L., Ju, X., Jia, M., Liu, H., Cao, W., Yu, P., Li, H., & Ren, X. (2021). Insights into forsythia honeysuckle (Lianhuaqingwen) capsules: A Chinese herbal medicine repurposed for COVID-19 pandemic. *Phytomedicine Plus*, *1*(2), Article 100027. https://doi.org/10.1016/j.phyplu.2021.100027

Liu, Z., Cheng, Y., Xiang, Y., & Chao, Z. (2024). Unveiling the potential applications of buds of *Lonicera japonica* Thunb. var. chinensis (Wats.) Bak based on *in vitro* biological activities, bio-active components and potential applications coupled to targeted metabolomics. *Frontiers in Plant Science*, 15, Article 1418957. https://doi.org/10.3389/fpls.2024.1418957

Liu, C., Liang, J.-P., Huang, X.-L., Liu, Z., Zhang, A.-B., Deng, N.-G., Wei, Z.-F., & Wang, J. (2023). Nerve growth factor causes epinephrine release dysfunction by regulating phenotype alterations and the function of adrenal medullary chromaffin cells in mice with allergic rhinitis. *Molecular Medicine Reports*, *27*(2), 39. https://doi.org/10.3892/mmr.2023.12926

Mengi, E., Kara, C. O., Alptürk, U., & Topuz, B. (2022). The effect of face mask usage on the allergic rhinitis symptoms in patients with pollen allergy during the COVID-19 pandemic. *American Journal of Otolaryngology*, *43*(1), Article 103206. https://doi.org/10.1016/j.amjoto.2021.103206

Moulik, S., Karmakar, J., Joshi, S., Dube, A., Mandal, C., & Chatterjee, M. (2021). Status of IL-4 and IL-10 driven markers in experimental models of Visceral leishmaniasis. *Parasite Immunology*, *43*(1), Article e12783. https://doi.org/10.1111/pim.12783

Oh, J.-H., Kim, S.-H., Kwon, O.-K., Kim, J.-H., Oh, S.-R., Han, S.-B., Park, J.-W., & Ahn, K.-S. (2022). Purpurin suppresses atopic dermatitis via TNF-α/IFN-γ-induced inflammation in HaCaT cells. *International Journal of Immunopathology and Pharmacology*, 36, Article 3946320221111135. https://doi.org/10.1177/03946320221111135

Piao, C. H., Fan, Y., Nguyen, T. V., Shin, H. S., Kim, H. T., Song, C. H., & Chai, O. H. (2021). PM2.5 exacerbates oxidative stress and inflammatory response through the Nrf2/NF-κB signaling pathway in OVA-induced allergic rhinitis mouse model. *International Journal of Molecular Sciences*, *22*(15), 8173. https://doi.org/10.3390/ijms22158173

Piao, C. H., Song, C. H., Lee, E. J., & Chai, O. H. (2020). Saikosaponin A ameliorates nasal inflammation by suppressing IL-6/ROR-γt/STAT3/IL-17/NF-κB pathway in OVA-induced allergic rhinitis. *Chemico-Biological Interactions*, 315, Article 108874. https://doi.org/10.1016/j.cbi.2019.108874

Piekarska, J., Madej, J. P., Gorczykowski, M., & Szczypka, M. (2023). The effects of honeysuckle (*Lonicera caerulea* L.) berry iridoid-anthocyanin extract on the intestinal and muscle histopathology in mice during experimental trichinellosis. *Molecules*, *28*(20), 7067. https://doi.org/10.3390/molecules28207067

Pimpley, V., Patil, S., Srinivasan, K., Desai, N., & Murthy, P. S. (2020). The chemistry of chlorogenic acid from green coffee and its role in attenuation of obesity and diabetes. *Preparative Biochemistry and Biotechnology*, *50*(10), 969–978. https://doi.org/10.1080/10826068.2020.1786699

Ren, Q., Guo, F., Tao, S., Huang, R., Ma, L., & Fu, P. (2020). Flavonoid fisetin alleviates kidney inflammation and apoptosis via inhibiting Src-mediated NF-κB p65 and MAPK signaling pathways in septic AKI mice. *Biomedicine and Pharmacotherapy*, 122, Article 109772. https://doi.org/10.1016/j.biopha.2019.109772

Sacchetti, M., Segatto, M., Bruscolini, A., Abicca, I., Cavaliere, C., & Lambiase, A. (2019). Changes of NGF pathway in allergic rhinoconjunctivitis: A conjunctival allergen challenge study. *Allergy*, *74*(3), 605–607. https://doi.org/10.1111/all.13641

Saleh, I. A., Vinatoru, M., Mason, T. J., Abdel-Azim, N. S., Aboutabl, E. A., & Hammouda, F. M. (2016). A possible general mechanism for ultrasound-assisted extraction (UAE) suggested from the results of UAE of chlorogenic acid from *Cynara scolymus* L. (artichoke) leaves. *Ultrasonics Sonochemistry*, *31*, 330–336. https://doi.org/10.1016/j.ultsonch.2016.01.002

Siddiqui, Z. A., Walker, A., Pirwani, M. M., Tahiri, M., & Syed, I. (2022). Allergic rhinitis: Diagnosis and management. *British Journal of Hospital Medicine*, *83*(2), 1–9. https://doi.org/10.12968/hmed.2021.0570

Tewari, D., Patni, P., Bishayee, A., Sah, A. N., & Bishayee, A. (2022). Natural products targeting the PI3K-Akt-mTOR signaling pathway in cancer: A novel therapeutic strategy. *Seminars in Cancer Biology*, *80*, 1–17. https://doi.org/10.1016/j.semcancer.2019.12.008

Tian, B., Ma, X., & Jiang, R. (2023). Daphnetin mitigates ovalbumin-induced allergic rhinitis in mice by regulating Nrf2/HO-1 and TLR4/NF-kB signaling. *American Journal of Rhinology and Allergy*, *37*(1), 19–25. https://doi.org/10.1177/19458924221124363

Tu, W., Chen, X., Wu, Q., Ying, X., He, R., Lou, X., Yang, G., Zhou, K., & Jiang, S. (2020). Acupoint application inhibits nerve growth factor and attenuates allergic inflammation in allergic rhinitis model rats. *Journal of Inflammation*, *17*, 4. https://doi.org/10.1186/s12950-020-0236-9

Velasco, E., Delicado-Miralles, M., Hellings, P. W., Gallar, J., Van Gerven, L., & Talavera, K. (2022). Epithelial and sensory mechanisms of nasal hyperreactivity. *Allergy*, *77*(5), 1450–1463. https://doi.org/10.1111/all.15259

Wang, H., Tian, L., Han, Y., Ma, X., Hou, Y., & Bai, G. (2022). Mechanism assay of honeysuckle for heat-clearing based on

metabolites and metabolomics. *Metabolites*, *12*(2), 121. https://doi.org/10.3390/metabo12020121

Wang, R., Yang, T., Feng, Q., Jiang, Y., Yuan, X., Zhao, L., Liu, N., Liu, Z., Zhang, Y., Wang, L., Cheng, G., Yao, J., Sun, C., Zhang, G., & Gu, Q. (2024). Integration of network pharmacology and proteomics to elucidate the mechanism and targets of traditional Chinese medicine Biyuan Tongqiao granule against allergic rhinitis in an ovalbumin-induced mice model. *Journal of Ethnopharmacology*, *318*(A), Article 116816. https://doi.org/10.1016/j.jep.2023.116816

Yu, H.-C., Huang, S.-M., Lin, W.-M., Kuo, C.-H., & Shieh, C.-J. (2019). Comparison of artificial neural networks and response surface methodology towards an efficient ultrasound-assisted extraction of chlorogenic acid from *Lonicera japonica*. *Molecules*, *24*(12), 2304. https://doi.org/10.3390/molecules24122304

Yu, H., Lin, L., Zhang, Z., Zhang, H., & Hu, H. (2020). Targeting NF-κB pathway for the therapy of diseases: Mechanism and clinical study. *Signal Transduction and Targeted Therapy*, *5*(1), 209. https://doi.org/10.1038/s41392-020-00312-6

Yuan, J., Liu, Y., Yu, J., Dai, M., Zhu, Y., Bao, Y., Peng, H., Liu, K., & Zhu, X. (2022). Gene knockdown of CCR3 reduces eosinophilic inflammation and the Th2 immune response by inhibiting the PI3K/AKT pathway in allergic rhinitis mice. *Scientific Reports*, *12*(1), 5411. https://doi.org/10.1038/s41598-022-09467-4

Zang, Z., Li, L., Yang, M., Zhang, H., Naeem, A., Wu, Z., Zheng, Q., Song, Y., Tao, L., Wan, Z., Zhang, Y., Leng, J., Liao, Z., & Guan, Y. (2024). Study on the ameliorative effect of honeysuckle on DSS-induced ulcerative colitis in mice. *Journal of Ethnopharmacology*, 325, Article 117776. https://doi.org/10.1016/j.jep.2024.117776

Zeng, Q., Luo, X., Tang, Y., Liu, W., & Luo, R. (2020). Leptin regulated ILC2 cell through the PI3K/AKT pathway in allergic rhinitis. *Mediators of Inflammation*, *2020*, Article 4176082. https://doi.org/10.1155/2020/4176082

Zheng, S.-L., Wang, Y.-M., Chi, C.-F., & Wang, B. (2024). Chemical characterization of honeysuckle polyphenols and their alleviating function on ultraviolet B-damaged HaCaT cells by modulating the Nrf2/NF-κB signaling pathways. *Antioxidants*, *13*(3), 294. https://doi.org/10.3390/antiox13030294